Abbreviations

SLE: Systemic lupus erythematosus; ESR: Erythrocyte sedimentation rate; CRP: C-reactive protein; CH50: Total complement activity; CT: Computed tomography; FFP: Fresh frozen plasma.

Competing interests

The authors have nothing to disclose.

Authors' contributions

YH drafted the manuscript, and participated in treatment. JS, KA, and TK carried out the clinical treatment and helped draft the manuscript. MH, EK, and HK analyzed the complement systems and interpreted the data. HT, MI, TH, and OO sequenced the *C1q* genes and performed reverse transcriptase-polymerase chain reaction analysis of *C1qB* mRNA. All authors read and approved the final manuscript.

Acknowledgement

We thank Edanz (http://www.edanzediting.co.jp) for English writing assistance.

Author details

[1]Department of Pediatrics, National Hospital Organization Okayama Medical Center, 1711-1 Tamasu, Kita-ku, Okayama 701-1192, Japan. [2]Department of Medical Technology Faculty of Health Sciences, Kobe Tokiwa University, 2-6-2 Ohtanicho, Nagata-ku, Kobe 653-0838, Japan. [3]Department of Pediatrics, Graduate School of Medical Sciences, Kyushu University, 3-1-1 Maidashi, Higasi-ku, Fukuoka 812-8582, Japan. [4]Department of Human Genome Technology, Kazusa DNA Research Institute, 2-6-7 Kazusakamatari, Chiba 292-0818, Japan. [5]Department of Dermatology, National Hospital Organization Okayama Medical Center, 1711-1 Tamasu, Kita-ku, Okayama 701-1192, Japan.

Received: 13 August 2013 Accepted: 25 October 2013
Published: 28 October 2013

References

1. Kishore U, Reid KB: **C1q: structure, function, and receptors.** *Immunopharmacology* 2000, **49**:159–170.
2. Walport MJ, Davies KA, Botto M: **C1q and systemic lupus erythematosus.** *Immunobiology* 1998, **199**:265–285.
3. Walport MJ: **Complement and systemic lupus erythematosus.** *Arthritis Res* 2002, **4**(Suppl 3):279–293.
4. Al-Mayouf SM, Abanomi H, Eldali A: **Impact of C1q deficiency on the severity and outcome of childhood systemic lupus erythematosus.** *Int J Rheum Dis* 2011, **14**:81–85.
5. Pickering MC, Botto M, Taylor PR, Lachmann PJ, Walport MJ: **Systemic lupus erythematosus, complement deficiency, and apoptosis.** *Adv Immunol* 2000, **76**:227–324.
6. McAdam RA, Goundis D, Reid KB: **A homozygous point mutation results in a stop codon in the C1q B-chain of a C1q-deficient individual.** *Immunogenetics* 1988, **27**:259–264.
7. Schejbel L, Skattum L, Hagelberg S, Åhlin A, Schiller B, Berg S, Genel F, Truedsson L, Garred P: **Molecular basis of hereditary C1q deficiency–revisited: identification of several novel disease-causing mutations.** *Genes Immun* 2011, **12**:626–634.
8. Namjou B, Keddache M, Fletcher D, Dillon S, Kottyan L, Wiley G, Gaffney PM, Wakeland BE, Liang C, Wakeland EK, Scofield RH, Kaufman K, Harley JB: **Identification of novel coding mutation in C1qA gene in an African-American pedigree with lupus and C1q deficiency.** *Lupus* 2012, **21**:1113–1118.
9. Topaloglu R, Taskiran EZ, Tan C, Erman B, Ozaltin F, Sanal O: **C1q deficiency: identification of a novel missense mutation and treatment with fresh frozen plasma.** *Clin Rheumatol* 2012, **31**:1123–1126.
10. Kobayashi E, Kitano E, Kitamura H: **A novel assay for serum complement activity: C42 generation assay.** *Int Arch Allergy Immunol* 1999, **120**:71–77.
11. Kitamura H, Nishimukai H, Sano Y, Nagaki K: **Study on C3-like factor in the serum of a C3-deficient subject.** *Immunology* 1984, **51**:239–245.
12. Kitano E, Kitamura H: **Dual effects of TNF on synthesis of complement components by a gastric cancer-derived cell line, KATO-III.** *Int Arch Allergy Immunol* 1999, **119**:54–59.
13. Whaley K, North J: **Haemolytic assays for whole complement activity and individual components.** In *Complement: A Practical Approach.* Edited by Dodds AW, Sim RB. Oxford: IRL Press; 1997:19–47.
14. Yurasov S, Wardemann H, Hammersen J, Tsuiji M, Meffre E, Pascual V, Nussenzweig MC: **Defective B cell tolerance checkpoints in systemic lupus erythematosus.** *J Exp Med* 2005, **201**:703–711.
15. Santer DM, Hall BE, George TC, Tangsombatvisit S, Liu CL, Arkwright PD, Elkon KB: **C1q deficiency leads to the defective suppression of IFN-alpha in response to nucleoprotein containing immune complexes.** *J Immunol* 2010, **185**:4738–4749.
16. Naito AT, Sumida T, Nomura S, Liu ML, Higo T, Nakagawa A, Okada K, Sakai T, Hashimoto A, Hara Y, Shimizu I, Zhu W, Toko H, Katada A, Akazawa H, Oka T, Lee JK, Minamino T, Nagai T, Walsh K, Kikuchi A, Matsumoto M, Botto M, Shiojima I, Komuro I: **Complement C1q activates canonical Wnt signaling and promotes aging-related phenotypes.** *Cell* 2012, **149**:1298–1313.
17. Manicassamy S, Reizis B, Ravindran R, Nakaya H, Salazar-Gonzalez RM, Wang YC, Pulendran B: **Activation of beta-catenin in dendritic cells regulates immunity versus tolerance in the intestine.** *Science* 2010, **329**:849–853.
18. Xu Y, Banerjee D, Huelsken J, Birchmeier W, Sen JM: **Deletion of beta-catenin impairs T cell development.** *Nat Immunol* 2003, **4**:1177–1182.
19. Nishino H, Shibuya K, Nishida Y, Mushimoto M: **Lupus erythematosus-like syndrome with selective complete deficiency of C1q.** *Ann Intern Med* 1981, **95**:322–324.
20. Uenaka A, Akimoto T, Aoki T, Tsuyuguchi I, Nagaki K: **A complete selective C1q deficiency in a patient with discoid lupus erythematosus (DLE).** *Clin Exp Immunol* 1982, **48**:353–358.
21. Orihara T, Tsuchiya K, Yamasaki S, Furuya T: **Selective C1q deficiency in a patient with systemic lupus erythematosus.** *Br J Dermatol* 1987, **117**:247–254.
22. Hayakawa J, Migita M, Ueda T, Itoh Y, Fukunaga Y: **Infantile case of early manifestation of SLE-like symptoms in complete C1q deficiency.** *J Nippon Med Sch* 2011, **78**:322–328.
23. Vassallo G, Newton RW, Chieng SE, Haeney MR, Shabani A, Arkwright PD: **Clinical variability and characteristic autoantibody profile in primary C1q complement deficiency.** *Rheumatology (Oxford)* 2007, **46**:1612–1614.
24. Mehta P, Norsworthy PJ, Hall AE, Kelly SJ, Walport MJ, Botto M, Pickering MC: **SLE with C1q deficiency treated with fresh frozen plasma: a 10-year experience.** *Rheumatology (Oxford)* 2010, **49**:823–824.
25. Cortes-Hernandez J, Fossati-Jimack L, Petry F, Loos M, Izui S, Walport MJ, Cook HT, Botto M: **Restoration of C1q levels by bone marrow transplantation attenuates autoimmune disease associated with C1q deficiency in mice.** *Eur J Immunol* 2004, **34**:3713–3722.
26. Bowness P, Davies KA, Norsworthy PJ, Athanassiou P, Taylor-wiedeman J, Borysiewicz LK, Meyer PAR, Walport MJ: **Hereditary C1q deficiency and systemic lupus erythematosus.** *QJM* 1994, **87**:455–464.

doi:10.1186/1546-0096-11-41
Cite this article as: Higuchi *et al.*: The identification of a novel splicing mutation in *C1qB* in a Japanese family with C1q deficiency: a case report. *Pediatric Rheumatology* 2013 **11**:41.

Tsuzuki et al. SpringerPlus 2013, 2:434
http://www.springerplus.com/content/2/1/434

SpringerPlus
a SpringerOpen Journal

SHORT REPORT Open Access

A Japanese neonatal case of glucose-6-phosphate dehydrogenase deficiency presenting as severe jaundice and hemolytic anemia without apparent trigger

Shinya Tsuzuki[1*], Moe Akahira-Azuma[1], Masao Kaneshige[1], Kazuhiro Shoya[1], Shinichi Hosokawa[1], Hitoshi Kanno[2] and Takeji Matsushita[1]

Abstract

Background: Glucose-6-phosphate dehydrogenase (G6PD) deficiency is rare among Japanese ethnicity although it is known as one of the most common hereditary disorders of erythrocytes, causing intravascular hemolysis. It is well-known that G6PD deficiency may cause hemolysis even in the neonatal period. However, most cases are asymptomatic, and the frequency of severe anemia is low.

Findings: We describe a Japanese male neonatal case of G6PD deficiency presenting as severe, persistent indirect hyperbilirubinemia on day 2 and hemolytic anemia. He was born to non-consanguineous Japanese parents without any family history. We could not find any triggers that could have induced hemolysis during pregnancy.

Conclusions: This case encouraged us to investigate G6PD deficiency as a differential diagnosis of severe neonatal jaundice and hemolytic anemia despite the low prevalence in Japan.

Keywords: Glucose-6-phosphate dehydrogenase deficiency; Neonate; Jaundice; Hemolytic anemia

Introduction

Glucose-6-phosphate dehydrogenase (G6PD) deficiency is said to be a rare disorder in Japan (Nakashima et al. 1977), even though it is one of the most common genetic enzymatic disorders in the world (Steiner & Gallagher 2007). The characteristic normal course of most G6PD-deficient children includes no symptoms throughout their life, and severe hyperbilirubinemia and kernicterus are seldom observed in the newborn period (Cappellini & Fiorelli 2008). In addition, acute severe hemolysis is thought to occur with the presence of triggering factors, such as infection, drugs, and fava beans (Cappellini & Fiorelli 2008; WHO Working Group 1989; Kaplan et al. 1998).

We describe a neonatal case of G6PD deficiency that developed severe jaundice and acute hemolytic anemia in the absence of ABO incompatibilities. The patient was successfully treated and avoided complications.

Case report

A male neonate was born at 38+5 weeks gestation to a 40-year-old gravida 2, para 2, blood group O Rh positive mother, via spontaneous vaginal delivery. The pregnancy was uncomplicated. Both his mother and father were non-consanguineous Japanese parents without any past medical history. His sibling (2-year-old girl) did not have any jaundice. His birth weight was 3460 g (appropriate for gestational age), and his Apgar score were 9 at 1 min and 9 at 5 min. He was exclusively breastfed, although the mother's breast milk secretion was not sufficient.

On day 2, he looked icteric, and a blood test was performed. His serum total bilirubin (STB) was 20.1 mg/dl (the indication of phototherapy according to the criteria of Kobe University, Japan: 12 mg/dl) (Department of Pediatrics, Kobe University Graduate School of Medicine 1993), his serum direct bilirubin was 1.29 mg/dl (normal

* Correspondence: shinyatsuzuki@yahoo.co.jp
[1]Department of Pediatrics, National Center for Global Health and Medicine (NCGM), 1-21-1 Toyama, Shinjuku-ku, 162-0855 Tokyo, Japan
Full list of author information is available at the end of the article

upper limit: 0.6 mg/dl). He was transferred to our NICU due to severe jaundice and was admitted on the same day.

Physical examinations revealed a body weight of 3217 g (7.0% weight loss). His vital signs were within normal limits. His bulbar conjunctiva and skin were icteric, and no hepatosplenomegaly was found. His blood type was group B, Rh positive. A complete blood count (CBC) revealed hemoglobin (Hb) of 12.6 g/dl and, a reticulocyte count of 10.9%; a blood smear for red cell morphology was within normal limits, without spherocytosis or red cell fragments. Chemistry showed no abnormal findings, except for STB (18.7 mg/dl). Direct and indirect Coombs' tests were negative. Blood culture was negative. Urinalysis did not show any occult blood, urobilinogen or bacteria. Chest and abdominal radiographs were normal. Head ultrasonography (US) showed no intracranial hemorrhage and abdominal US did not reveal any adrenal hemorrhage.

An exchange transfusion was reserved because of the patient's STB (the criteria for indication was an STB>20 mg/dl, according to Kobe University), and phototherapy was initiated. Table 1 shows the course of the blood test results and management. A total of 15 ml/kg of red blood cells (RBCs) was transfused on 2 consecutive days (days 16 and days 17). After the RBCs transfusion, a CBC showed 14.3 g/dl of Hb. On day 16, an erythrocyte osmotic fragility test, CD55 and CD59 were within normal limits. He was referred to Tokyo Women's Medical University to further investigate any erythrocyte disorders. His glucose-6-phosphate dehydrogenase activity was 3.06 IU/gHb (his father and mother's activity was not available), while the normal level is 11.0 IU/gHb. The patient was diagnosed as having a G6PD deficiency. Two weeks after birth, his jaundice and anemia became stable without any treatment and he was discharged on day 21 with an STB value of 14.7 mg/dl, Hb of 12.9 g/dl and a reticulocyte count of 2.0%.

Discussion

We treated a Japanese male with severe and refractory jaundice and progressive, early onset normocytic anemia born to non-consanguineous parents. The signs of hemolysis were obscure at the onset of jaundice. Rh, ABO compatibilities and spherocytosis were not observed. Because the erythrocyte enzyme test is not easily accessible in Japan, the infant was referred to a specific institute, and was eventually diagnosed as having a G6PD deficiency on day 75. The instructive aspects of the present report are as follows. First, although G6PD deficiency is uncommon in Japan, the patient was born to Japanese parents. Second, the case presented as severe jaundice and hemolytic anemia, although most cases are asymptomatic, particularly in the neonatal period. Third, he apparently did not have any triggers for an acute episode of hemolysis.

The prevalence of G6PD deficiency is estimated at approximately 0.1% in Japan (Nakashima et al. 1977). In most hemolytic cases, it was inferred that the mothers were of non-Japanese ethnicity because gene variants found in Japan were not associated with severe hemolytic anemia (Nakashima et al. 1977). This also might be attributed to the fact that the incidence of gene mutation was quite different from southern Chinese in the Taiwan-Hakka population and Philippines (5.5% and 6.0% each) (Nakashima et al. 1977). In fact, case reports of G6PD deficiency with severe hemolytic anemia published in Japan often describe the family history of foreign mothers (Shimomura et al. 2002; Akazawa et al. 2011). Therefore this case was also characteristic in the point that both the father and mother are Japanese.

Most G6PD-deficient individuals are entirely asymptomatic (Mehta 1994). The most common clinical manifestation in the neonatal period is neonatal jaundice, and acute hemolytic anemia is usually rare; this is because neonatal jaundice due to G6PD deficiency is not due to

Table 1 Serum bilirubin, hematological values and other managements during hospitalization

DOL	2	5	9	13	16	17	31	75	94	149
Blood Test										
Hb (g/dl)	12.6	12.0	9.4	8.6	7.0	14.3	10.8	8.4	7.9	9.1
Hct (%)	37.1	35.6	28.1	25.5	20.6	40.8	31.4	24.1	23.7	28.1
Ret (%)	10.9	5.4	2.5	4.1	4.0	2.2	0.5	4.6	7.5	8.6
STB (mg/dl)	18.7	18.5	14.4	19.2	14.7	14.6	13.9	4.2	2.0	2.0
Management										
Phototherapy†	+	+	-	+	-	-	-	-	-	-
Transfusion					*	*				
Other tests‡					+			+		

Abbreviations: *DOL* Day of life, *Hb* Hemoglobin, *Hct* Hematocrit, *Ret* Reticulocyte, *STB* Serum total bilirubin.
† treatment with phototherapy is indicated with a +.
‡ an osmotic fragility test was performed on DOL 16; an erythrocyte enzyme test was performed on DOL 75.

hemolysis, and hyperbilirubinemia is thought to be secondary to reduced hepatic conjugation and bilirubin excretion (Cappellini & Fiorelli 2008; Beutler 1994; Kaplan & Hammerman 2002). Our case presented neonatal jaundice in advance of the hemolytic anemia; however, the increased reticulocyte count on day 2 suggests that both hyperbilirubinemia and hemolysis may occur simultaneously. Kawaguchi et al. also reported a suspected antenatal hemolysis case in Japan (Kawaguchi et al. 1997). In this case, an extremely high reticulocyte level (344‰) was presented, and intrauterine hemorrhage was strongly suspected. They attributed the early onset hemolysis to oxidative stress as a result of maternal history of the common cold or drug use.

This illness generally manifests as acute hemolysis in childhood, which usually arises when red blood cells undergo oxidative stress triggered by infection or the ingestion of fava beans. Despite conducting a thorough and precise interview, we could not identify any history of drug or food intake during the pregnancy. There have been a few G6PD deficiency cases presenting acute hemolysis in the absence of any trigger that have also been reported in the literature (Dhillon et al. 2003; Shah & Yeo 2007). Our case supports the theory that massive hemolysis may occur in neonates with G6PD deficiency even in the absence of obvious triggering factors.

The abnormal genetic mutations of this disease are classified into 3 categories. Class V/IV is clinically asymptomatic, and class III/II (the border between III and II is not obvious) is basically asymptomatic; both are without the risk of hemolytic anemia and neonatal jaundice. Class I presents (severe) neonatal jaundice and acute exacerbation of hemolytic anemia (WHO Working Group 1989). The limitation of our report is that this case should be classified as class I because the patient showed both acute and chronic hemolytic episodes. However, no genetic testing has been performed. Differences in the clinical course due to genetic transmutation may be present in this disorder. Therefore, genetic testing is one of important part of the management of G6PD patients.

The Japanese male neonate with G6PD deficiency in this report simultaneously presented with severe jaundice and acute hemolysis. Given the lack of family history, triggers, definite laboratory data, and rare disease status among patients with Japanese ethnicity, we recommend further investigation for G6PD deficiency in cases of neonatal hemolytic anemia complicated with jaundice.

Abbreviations

G6PD: Glucose-6-phosphate dehydrogenase; STB: Serum total bilirubin; CBC: Complete blood count; Hb: Hemoglobin; US: Ultrasonography; RBCs: Red blood cells.

Competing interest

The authors declared no potential conflicts of interest with respect to the research, authorship, and/or publication of this article.

Authors' contribution

The corresponding author ST wrote the main manuscript text. MAA and MK proofread our report and revising it critically. HK carried out the erythrocyte enzyme test and greatly contributed to diagnose this case. SH and KS prepared the table. All authors read and approved the final manuscript.

Author details

[1]Department of Pediatrics, National Center for Global Health and Medicine (NCGM), 1-21-1 Toyama, Shinjuku-ku, 162-0855 Tokyo, Japan. [2]Department of Transfusion Medicine and Cell Processing, Tokyo Women's Medical University, Tokyo, Japan.

Received: 8 March 2013 Accepted: 2 September 2013
Published: 4 September 2013

References

Akazawa Y et al (2011) A case of glucose-6-phosphate dehydrogenase deficiency with acute hemolytic anemia. J Japan Soc Premature Newborn Med 23:108–123
Beutler E (1994) G6PD deficiency. Blood 84:3613–3636
Cappellini MD, Fiorelli G (2008) Glucose-6-phosphate dehydrogenase deficiency. Lancet 371:64–74
Department of Pediatrics, Kobe University Graduate School of Medicine (1993) The management of preterm neonates. Nihon Shoni Iji Syuppansya, Tokyo, pp 205–224
Dhillon AS et al (2003) Massive acute haemolysis in neonates with glucose-6-phosphate dehydrogenase deficiency. Arch Dis Child Fetal Neonatal Ed 88:F534–F536
Kaplan M, Hammerman C (2002) Glucose-6-phosphate dehydrogenase deficiency: a potential source of severe neonatal hyperbilirubinaemia and kernicterus. Semin Neonatol 7:121–128
Kaplan M et al (1998) Favism by proxy in nursing glucose-6-phosphate dehydrogenase deficient neonates. J Perinatol 18:477–479
Kawaguchi A et al (1997) Antenatal haemolytic anemia of glucose-6-phosphate dehydrogenase deficiency: a case report. J Japan Soc Perinat Neonatal Med 43:148–151
Mehta AB (1994) Glucose-6-phosphate dehydrogenase deficiency. Postgrad Med J 70:871–877
Nakashima K et al (1977) G6PD Ube, a glucose-6-phosphate dehydrogenase variant found in four unrelated Japanese families. Am J Hum Genet 29:24–30
Shah VA, Yeo CL (2007) Massive acute haemolysis and severe neonatal hyperbilirubinemia in glucose-6-phosphate dehydrogenase-deficient preterm triplets. J Paediatr Child Health 43:411–413
Shimomura Y et al (2002) A case of glucose-6-phosphate dehydrogenase deficiency with acute hemolysis episode caused by infection. Jpn J Pediatr 55:203–206
Steiner LA, Gallagher PG (2007) Erythrocyte disorders in the perinatal period. Semin Perinatol 31:254–261
WHO Working Group (1989) Glucose-6-phosphate dehydrogenase deficiency. Bull WHO 67:601–611

doi:10.1186/2193-1801-2-434
Cite this article as: Tsuzuki *et al.*: A Japanese neonatal case of glucose-6-phosphate dehydrogenase deficiency presenting as severe jaundice and hemolytic anemia without apparent trigger. *SpringerPlus* 2013 **2**:434.

ELSEVIER

Brain & Development 35 (2013) 349–355

BRAIN & DEVELOPMENT
Official Journal of the Japanese Society of Child Neurology

www.elsevier.com/locate/braindev

Original article

Enhanced expression of myogenic differentiation factors and skeletal muscle proteins in human amnion-derived cells via the forced expression of *MYOD1*

Yoshika Akizawa [a,b], Hitoshi Kanno [a,c], Yayoi Kawamichi [b], Yoshio Matsuda [b], Hiroaki Ohta [d], Hisaichi Fujii [c], Hideo Matsui [b], Kayoko Saito [a,*]

[a] *Institute of Medical Genetics, Tokyo Women's Medical University, Tokyo, Japan*
[b] *Department of Obstetrics and Gynecology, Tokyo Women's Medical University, Tokyo, Japan*
[c] *Department of Transfusion Medicine and Cell Processing, Tokyo Women's Medical University, Tokyo, Japan*
[d] *Sanno Medical Center, International University of Health and Welfare, Japan*

Received 15 December 2011; received in revised form 12 May 2012; accepted 21 May 2012

Abstract

Objectives: Mesenchymal stem cells are expected to be an ideal cell source for cellular and gene therapy. We previously showed that cells derived from the human placenta can be induced to differentiate into myotubes *in vitro* and to express dystrophin in mdx/scid mice *in vivo*. In this study, we examined whether amnion-derived cells can be efficiently transduced and differentiated using lentiviral vectors carrying human *MYOD1*. *Methods:* The amnion-derived cells were isolated from human preterm placentas. They were transduced with the *MYOD1* vector, and mRNA levels for *MYOD1*, *MYF5*, *MYOG*, *MYH2* and *DMD* were determined by quantitative-reverse transcriptase-polymerase chain reaction, and also examined immunocytochemically. *Results:* Approximately 70% of amnion-derived cells were efficiently transduced by the lentiviral vectors. *MYOD1* activates *MYF5* and *MYOG*, *MYH2* and *DMD* after a 7-day culture. The concerted upregulations of these myogenic regulatory factors enhanced *MYH2* and *DMD* expressions. *PAX7* was below the detectable level. Both myosin heavy chain and dystrophin were demonstrated by immunocytochemistry. *Conclusions:* *MYOD1* activates *MYF5* and *MYOG*, the transcription factor genes essential for myogenic differentiation, and the concerted upregulation of these myogenic regulatory factors enhanced *MYH2* and *DMD* expressions. The amniotic membrane is an immune-privileged tissue, making *MYOD1*-transduced amnion-derived cells an ideal cell source for cellular and gene therapy for muscle disorders. This is the first report showing that amnion-derived cells can be modified by exogenous genes using lentiviral vectors. Furthermore, *MYOD1*-transduced amnion-derived cells are capable of the dystrophin expression necessary for myogenic differentiation.

Keywords: Duchenne muscular dystrophy; Mesenchymal stem cell; Cellular therapy; Gene therapy; Dystrophin; Placenta

1. Introduction

Duchenne muscular dystrophy (OMIM# 310200) is an X-linked recessive inherited disorder that affects 1 in 3500 males. The onset of Duchenne muscular dystrophyis usually before the age of 3 years, and patients die of respiratory failure around the age of 20 [1]. Duchenne muscular dystrophyis caused by structural mutations in

* Corresponding author. Address: Institute of Medical Genetics, Tokyo Women's Medical University, 10-22 Kawada-cho, Shinjyuku-ku, Tokyo 162-0054, Japan. Tel.: +81 3 3353 8111; fax: +81 3 5269 7689.
E-mail address: saito@img.twmu.ac.jp (K. Saito).

0387-7604/$ - see front matter © 2012 The Japanese Society of Child Neurology. Published by Elsevier B.V. All rights reserved.
http://dx.doi.org/10.1016/j.braindev.2012.05.012

the dystrophin gene (*DMD*), which encodes dystrophin, a large membrane-associated protein that plays an important role in linking intracellular cytoskeletal actin filaments to the sarcolemmal membrane [2]. Approximately 60% of *DMD* mutations are large deletions or insertions, whereas 40% are nonsense, missense, or small insertion-deletion mutations.

No curative therapeutic approaches for Duchenne muscular dystrophy currently exist. However, cell-based treatments in addition to gene therapy [3], exon skipping therapy [4], and read-through therapy with aminoglycosides [5] remain promising options.

Mesenchymal stem cells (MSC) are expected to be an ideal cell source for cellular and gene therapy because they can easily be obtained from bone marrow, adipose tissues, and the placenta, they are abundant and non-tumorigenic, and they have the useful characteristics of homing and chemokine secretion. MSC are already utilized for the treatment of graft versus host disease [6] and inflammatory bowel disease [7]. Several laboratories have shown that MSC can be obtained from amnion-derived cells and induced to differentiate into myocytes [8].

Although the myogenic differentiation of MSC can be induced by treating them with demethylating agents such as 5-azacythidine (5AZA), there is no marked enhancement of either *MYOD1*, the human myogenic differentiation factor 1 gene, or *MYH2* expression, nor does5AZA treatment substantially increase the myogenic differentiation of MSC [9]. In addition, there have been several attempts to enhance the myogenesis by introducing *MYOD1* into cells [10]. It was recently shown that human adipose-derived cells displayed enhanced myogenic differentiation after being forced to express *MYOD1* [11], and another group showed that forced expression of *MYOD1* led to the trans-differentiation of human fibroblasts into myotubes [12].

In this study, we introduced human *MYOD1* into amnion-derived cells using a lentiviral vector and examined the precise gene expression levels of *MYF5*, *MYOG*, *MYH2* and *DMD*. We demonstrated significant upregulations of the genes for essential transcription factors involved in myogenesis. The potential applications of*MYOD1*-transduced amnion-derived cells are also discussed.

2. Materials and methods

2.1. Isolation of human amnion-derived cells

Ethics approval for the tissue collection was granted by the Institutional Review Board of Tokyo Women's Medical University, Japan. Written informed consent was obtained prior to sample collection. Amnion tissue samples were obtained from normal full-term pregnancies at the time of caesarean section before the onset of labor. None of these pregnancies were complicated by premature membrane rupture or chorioamnionitis. The placentas were processed within 24 h of collection; i.e., they were thoroughly washed with phosphate-buffered saline (a solution containing sodium chloride, sodium phosphate, potassium chloride and potassium phosphate), and, after separation from the placentas, the amnions were minced into 5 mm sections using knives on a clean bench. The amnion tissue was placed in collagen I coated dishes (Iwaki, Japan), and after 20 min, Mesenchymal Stem Cell Basal Medium (MSCBM, Lonza, USA) was carefully poured onto the attached cells, which were then maintained at 37 °C in 5% CO_2. After 48 h, the non-adherent cells were removed, and the medium was changed twice a week. After about one week, a few colonies were found in the dishes. At 70–80% confluence, the amnion-derived cells were harvested with 0.5% Trypsin–EDTA (Life Sciences, USA) and plated onto new dishes. Cells were processed from 24 placentas, and primary cultures from 8 placentas were used for this study.

2.2. Flowcytometric analysis

The amnion-derived cells were used for fluorescent activated cell sorting (FACS) analysis employing the EPICS ALTRA XL-MCL analyzer (Beckman Coulter, USA), and the data were analyzed with EXPO™32 ADC software (Beckman Coulter). Antibodies against human CD14, CD29, CD34, CD44, CD45, CD73, CD105, CD166, HLA-ABC, and HLA-DR were obtained from Beckman Coulter and BD Biosciences Pharmingen (USA), AbD Serotec (UK) and Cytognos (Spain).

2.3. Production of lentiviral vectors and MYOD1 transduction of human amnion-derived cells

A full-length human *MYOD1* cDNA clone (Genome Network Project Clone, WW01A62C23) was provided by the RIKEN Bioresource Center (Ibaraki, Japan) through the National Bio-Resource Project of the Ministry of Education, Culture, Sports, Science, and Technology (MEXT) of Japan [13–16]. A lentiviral vector carrying the *MYOD1* cDNA, pLenti6/human*MYOD1*, was constructed using the pLenti6/UbC/V5-DEST Gateway Vector kit and the ViraPower Lentiviral Expression System (Life Technologies, USA). A GFP expression vector, pRRL.PPT.SF.IRES-GFP, was kindly provided by Taiju Utsugisawa.

Three micrograms of the purified pLenti6/UbC/V5-DEST – human*MYOD1* cDNA and pRRL.PPT.SF.IRES-GFP were used for the transfection of 4×10^6 293FT cells together with Lipofectamine 2000 (provided with the kit) reagent and ViraPower packaging Mix (provided with the kit). After 48 h, the supernatant

was collected. Eight milliliters of viral supernatant were added to 6–8 × 10^5 amnion-derived cells. To examine the transfection efficiency of our procedure, the GFP expression of the cells was analyzed by FACS.

2.4. In vitro myogenesis

The amnion-derived cells were transduced with the pLenti6/UbC/V5-DEST – human *MYOD1* supernatant and seeded onto collagen I coated cell culture dishes (IWAKI) at a density of 1 × 10^4 per ml in growth medium (Dulbecco's Modified Eagle Medium (DMEM) supplemented with 20% fetal bovine serum) for 24 h. The cell cultures were then washed twice with phosphate-buffered saline (−), and maintained in differentiation medium (DMEM supplemented with 2% horse serum (Iwaki, Japan)). The medium was changed twice a week until completion of the experiment.

2.5. Quantitative-reverse transcriptase-polymerase chain reaction using MYOD1-transduced amnion-derived cells

Total RNA was purified from the *MYOD1*-transduced amnion-derived cells using the RNeasy mini kit (QIAGEN, Germany) at 7 and 14 days after transduction. Two micrograms of total RNA were subjected to reverse-transcription using Expand Reverse Transcriptase (Roche, USA). The gene expression levels of *MYOD1, MYF5, PAX7, MYOG, MYH2*, and *DMD* were analyzed using the quantitative-reverse transcriptase-polymerase chain reaction (Q-RT-PCR), the primers listed in Supplementary Table 1, and Mx3000™ (Stratagene, USA). The non-transduced amnion-derived cells were designated the day 0 cells. Q-RT-PCR was performed at 95 °C for 10 min for 45 cycles, with each cycle consisting of 95 °C for 15 s, followed by treatment at 60 °C for 60seconds after completion of the last cycle. Relative gene expression levels were calculated using RNA extracted from normal human skeletal muscle myoblast cells (Lonza), which had been cultured for 4–5 days using the SkGM-2 BulletKit (Lonza) or for 7 days in total DMEM supplemented with 2% horse serum as a myoblast control [17].

2.6. Immunocytochemical analysis

The cultures were fixed in 4% paraformaldehyde and stained with either a mouse anti-human dystrophin IgG1 monoclonal antibody (NCL-DYS2, Novocastra, UK) or a mouse anti-myosin heavy chain IgG2 monoclonal antibody (MF-20, Developmental Studies Hybridoma Bank, USA). The cells were visualized with appropriate AlexaFluor488 goat anti-mouse IgG secondary antibodies (Invitrogen, USA). Total cell nuclei were stained with Hoechst solution (Sigma Aldrich, UK).

3. Results

3.1. Morphology of the amnion-derived cells

We isolated amnion-derived cells from placentas, and a large number of primary cells were successfully obtained. These cells consisted of small fibroblast-like and cobblestone-like cells (Fig. 1a), and after 3 passages, they had formed a homogeneous population of the fibroblast-like cells (Fig. 1b). The yield was approximately 2 × 10^7 cells per gram of amnion tissue after three weeks.

3.2. Surface markers of amnion-derived cells

The surface marker expressions of amnion-derived cells were evaluated by flowcytometric analysis (Fig. 2). After 3 passages, the amnion-derived cells were positive for CD29, CD44, CD73, CD105, CD166, and HLA-ABC. However, they did not express any hematopoietic lineage markers such as CD34, CD14, CD45 or HLA-DR.

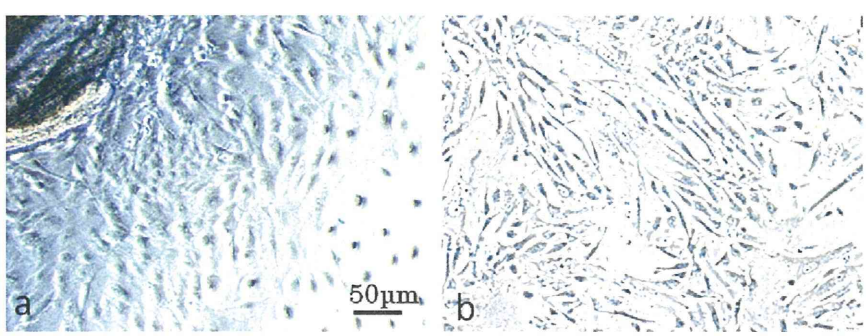

Fig. 1. Photomicrographs of amnion-derived cells in primary cultures in which two cell types, cobblestone- and fibroblast-like cells, can be seen (a). After three passages, the cells had formed a homogeneous population of fibroblast-like cells (b). Scale bar: 50 μm.

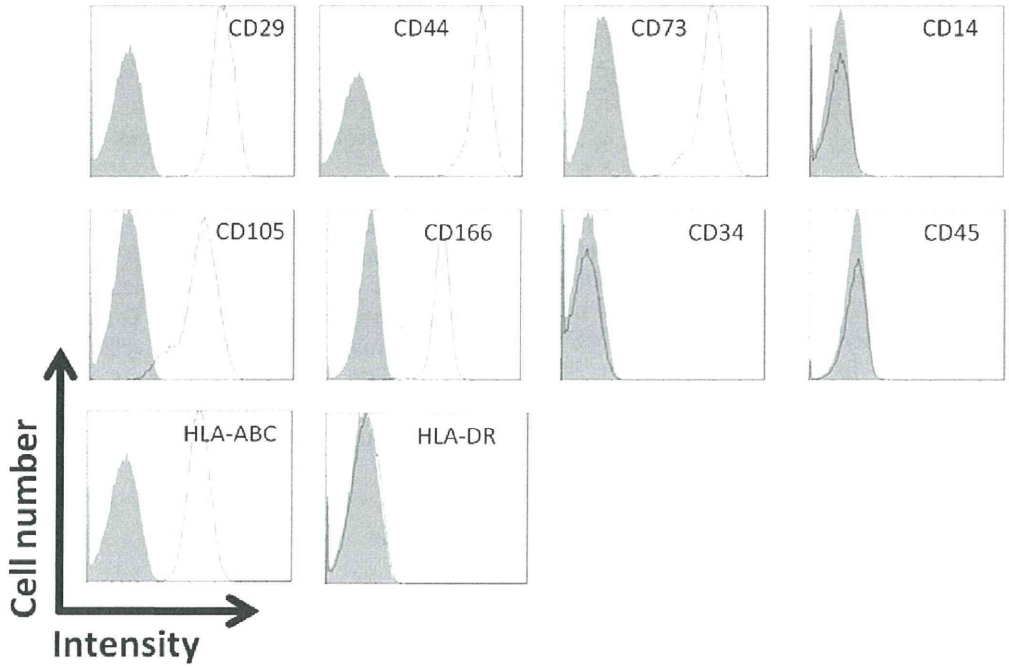

Fig. 2. Surface marker expressions of amnion-derived cells were evaluated by flowcytometric analysis after 3 passages. They expressed the following MSC markers: CD29, CD44, CD73, CD105 CD166, and HLA-ABC. However, they did not express any hematopoietic lineage markers such as CD34, CD14, CD45, or HLA-DR.

3.3. Transduction of amnion-derived cells with a GFP vector

The amnion-derived cells were transduced with a GFP vector, and the transduction efficiency of our procedure was evaluated by flowcytometric analysis after 72 h. In each experiment, approximately 70–80% of amnion-derived cells were positive for GFP (data not shown).

3.4. Q-RT-PCR of MYOD1 transduced amnion-derived cells

The mRNA levels of *MYOD1, MYF5, MYOG, PAX7, MYH2, and DMD* in the *MYOD1*-transduced amnion-derived cells were determined by Q-RT-PCR. Forced expression of human *MYOD1* in amnion-derived cells markedly enhanced their *MYF5* and *MYOG* gene expression levels after 7 days of culture (Fig. 3). On day 7, the *MYOD1*mRNA level of these cells was increased 50-fold as compared to that observed on day 0. The mRNA level corresponded to 4.8% of that in the control myoblasts. On day 14, the *MYOD1*mRNA level had decreased to 1.1% of that in the controls, suggesting that the enhanced *MYOD1* mRNA expression was transient.

It should be noted that *MYF5*gene expression was highly upregulated in the *MYOD1*-transduced amnion-derived cells. On day 7, it was increased by over 500-fold, and the relative mRNA level had reached 5.6% of that in control myoblasts. However, on day 14, the *MYF5* expression of these cells had been almost completely abrogated.

The *MYOG* mRNA level in the amnion-derived cells was extremely low (0.02%) on day 0. On day 7, it had reached 0.125% of that in the control myoblasts, but was undetectable by day14.

On days 7 and 14 the mRNA levels of *MYH2* were 0.11% and 0.33% and those of *DMD* were 20% and 28%, respectively, of corresponding levels in the control cells. These results suggest that genes encoding skeletal muscle proteins were activated following the concerted activation of myogenic regulatory factors such as *MYOD1*, *MYF5*, and *MYOG*. On the other hand, the level of *PAX7* was not measurable in either the non-transduced or transduced amnion-derived cells (data not shown).

3.5. Immunocytochemistry of myogenic differentiated cells

The MYOD1-transduced amnion-derived cells were subjected to immunocytochemical analysis after a 28-day culture in differentiation medium. Both myosin heavy chain 2 and dystrophin were immunologically detected in their cytosol and nuclei, suggesting these cells to be capable of differentiating into myotubes (Fig. 4).

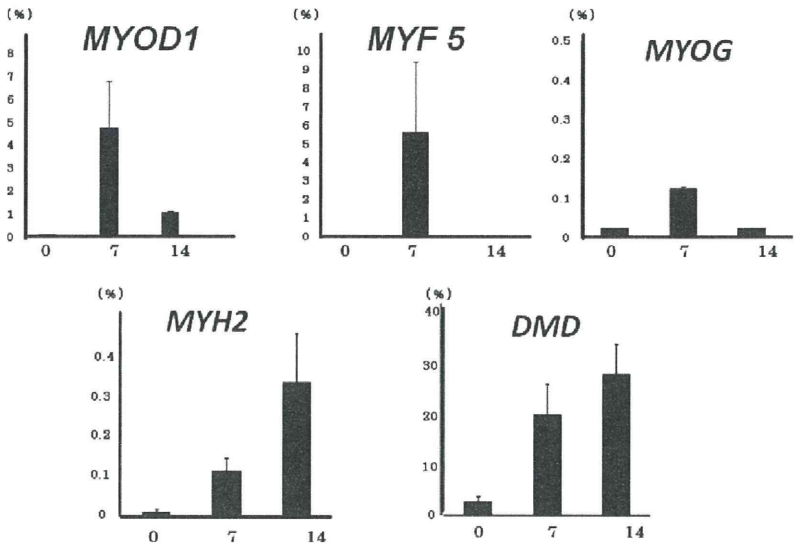

Fig. 3. The mRNA levels of *MYOD1, MYF5, MYOG, PAX7, MYH2*, and *DMD* in the *MYOD1* transduced amnion-derived cells were determined by Q-RT-PCR using the Universal Probe Library system (Roche). Relative gene expression levels were calculated using normal human skeletal muscle myoblast cells (Lonza) as a control. Day 0 represents the mRNA level of the amnion-derived cells on the day of transduction. Days 7 and 14 represent the mRNA levels of the *MYOD1*-transduced amnion-derived cells. The mRNA levels of the cells were as follows: *MYOD1*, 0.10 ± 0.05%, 4.8 ± 2.0%, and 1.09 ± 0.07%; *MYF5*, 0.013 ± 0.001%, 5.6 ± 3.8%, and < 0.0025%; *MYOG*, ≦0.00%, 0.13 ± 0.01%, and <0.0025%; MYH2, 0.01 ± 0.001%, 0.11 ± 0.03%, and 0.33 ± 0.12%; and *DMD*, 2.8 ± 1.0%, 20 ± 6.0%, and 28 ± 6.0%. The mRNA levels of the *MYOD1*-transduced amnion-derived cells were markedly upregulated, as shown in the figure; however, *PAX7* was not detected in either the untreated or the transduced amnion-derived cells.

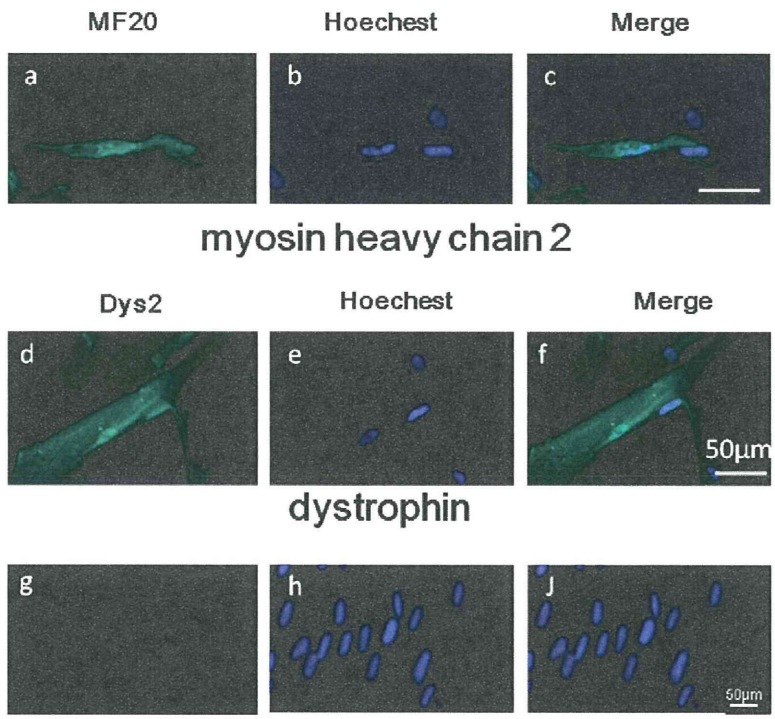

Fig. 4. Expressions of muscle specific genes during the differentiation of amnion-derived cells. *MYOD1*-transduced amnion-derived cells were cultured in differentiation medium for 28 days and stained using immunohistocytochemical methods. (a) Myosin heavy chain molecule (green, MF20); (b) nuclei (blue, Hoechst); (c) merged image of a and b; (d) dystrophin molecule (green, Dys2); (e) nuclei (blue, Hoechst); (f), merged image of d and e;The untreated amnion-derived cells expressed neither myosin heavy chain (g–h) nor dystrophin (data not shown). Scale bars: 50 μm.

4. Discussion

Myogenesis is classified into two modes, skeletal myogenic differentiation during development and regeneration mediated through satellite cells after injury. Previous studies have revealed that several transcription factors are essential for regulating embryonic and adult muscle formation. Among these factors, MyoD, Myf5, and myogenin are considered to be master transcription factors that are essential for myogenesis and are known as myogenic regulatory factors [18]. During myogenesis, *MYOD1* and *MYF5* are able to functionally substitute for one another [19]. In contrast, MyoD and Myf5 have distinct functions in the processes involved in recovery from muscle injury: MyoD is indispensable for the commitment of satellite cells to become myogenic precursor cells, and Myf5 plays an important role in myoblast proliferation [20]. On the other hand, myogenin is important for terminal muscle differentiation and lineage maintenance [21]. In this study, we clearly showed *MYOD1* transduction to activate both *MYF5* and *MYOG*, leading to myogenic differentiation resembling the developmental stages between myogenic progenitors and myoblasts. It is still unclear whether the concerted activation of *MYF5* and *MYOG* is due to direct transactivation by MyoD. Nonetheless, sequential activation of myogenic differentiation factors subsequently increased the gene expression levels of *MYH2* and *DMD*. As a result, the myosin heavy chain2 and dystrophin were immunocytochemically detected, as shown in Fig. 4. However, we were unable to demonstrate the protein expression of MYOD1, MYF5, MYOG, or PAX7, since examining the expressions of transcription factors by Western blotting or other immunological procedures is quite difficult.

Satellite cells, which are generated around myofibers during fetal development, express another transcription factor, Pax7. They are mitotically quiescent, but are activated in response to the stress induced by muscle injury [22]. Although the *MYOD1*-transduced amnion-derived cells did not display *PAX7* expression, the biological significance of this transcription factor remains obscure.

We previously demonstrated that human MSC transplanted into skeletal muscles of mdx mice successfully differentiated and fused with murine muscles, suggesting cellular therapy to be a promising strategy for Duchenne muscular dystrophy [23]. A previous report showed that dystrophin Dp71 and dystrophin-associated proteins are co-localized to the nuclei of muscle cells. This result implies that allogenic *MYOD1*-transduced amnion-derived cells would be a useful tool for cellular therapy [24].

The amniotic membrane is an immuno-privileged tissue and has been used as a biological membrane for treating burns, injuries, and skin ulcers as well as for corneal transplantation [25–27], and the transplantation of amniotic membrane-derived cells has been experimentally applied to the treatment of lung fibrosis [28]. Recently, a preclinical study reported their use for regenerative therapy targeting central nervous system tissues [29]. It is also known that the amniotic epithelium produces anti-inflammatory and growth factors that are beneficial for the treatment of inflammatory corneal diseases [30]. Taken together, these observations explain the increasing attention that the human amniotic membrane has received due to its anti-scarring, anti-inflammatory, and wound-healing properties, as well as its multipotent differentiation ability and immunomodulatory features [31].

In conclusion, the placenta has several advantages as the cellular source for devising novel cellular and gene therapies, especially for muscle disorders. The placenta can be obtained non-invasively, the amniotic membrane has been shown to be an immune-privileged tissue and *MYOD1*-transduced amnion-derived cells are capable of the dystrophin expression needed for myogenic differentiation.

Acknowledgements

We thank Ms. Takako Aoki for her excellent technical assistance. This work was supported by a Research Grant (20B-13-03) for Nervous and Mental Disorders from the Ministry of Health, Labor, and Welfare and Grants-in-Aid from the Research Committee of Spinal Muscular Atrophy (SMA) and the Ministry of Health, Labor, and Welfare of Japan. We would like to express our sincere thanks to Prof. Sumio Sugano of the University of Tokyo, Dr. Yoshihide Hayashizaki of RIKEN Omics Science Center, and the Research Association for Biotechnology for providing the *MYOD1* cDNA clone.

Appendix A. Supplementary data

Supplementary data associated with this article can be found, in the online version, at http://dx.doi.org/10.1016/j.braindev.2012.05.012.

References

[1] Nowak K, Davies KE. Duchenne muscular dystrophy and dystrophin: pathogenesis and opportunities for treatment. EMBO Rep 2004;5:872–6.
[2] Ahn AH, Kunkel LM. The structural and functional diversity of dystrophin. Nat Genet 1993;3:283–91.
[3] Wang B, Li J, Qiao C, Chen C, Hu P, Zhu X, et al. A canine minidystrophin is functional and therapeutic in mdx mice. Gene Ther 2008;15:1099–106.
[4] Matsuo M, Masumura T, Nishio H, Nakajima T, Kitoh Y, Takumi T, et al. Exon skipping during splicing of dystrophin

mRNA precursor due to an intraexon deletion in the dystrophin gene of Duchenne muscular dystrophy kobe. J Clin Invest 1991;87:2127–31.
[5] Barton-Davis ER, Cordier L, Shoturma DI, Leland SE, Sweeney HL. Aminoglycoside antibiotics restore dystrophin function to skeletal muscles of mdx mice. J Clin Invest 1999;104:375–81.
[6] Kebriaei P, Isola L, Bahceci E, Holland K, Rowley S, McGuirk J, et al. Adult human mesenchymal stem cells added to corticosteroid therapy for the treatment of acute graft-versus-host disease. Biol Blood Marrow Transplant 2009;15:804–11.
[7] Ko IK, Kim BG, Awadallah A, Mikulan J, Lin P, Letterio JJ, et al. Targeting improves MSC treatment of inflammatory bowel disease. Mol Ther 2010;18:1365–72.
[8] Portmann-Lanz CB, Schoeberlein A, Huber A, Sager R, Malek A, Holzgreve W, et al. Placental mesenchymal stem cells as potential autologous graft for pre- and perinatal neuroregeneration. Am J Obstet Gynecol 2006;194:664–73.
[9] Drost AC, Weng S, Feil G, Schäfer J, Baumann S, Kanz L, et al. In vitro myogenic differentiation of human bone marrow-derived mesenchymal stem cells as a potential treatment for urethral sphincter muscle repair. Ann NY Acad Sci 2009;1176: 135–43.
[10] Lattanzi L, Salvatori G, Coletta M, Sonnino C, Cusella De Angelis MG, Gioglio L, et al. High efficiency myogenic conversion of human fibroblasts by adenoviral vector-mediated MyoD gene transfer. An alternative strategy for ex vivo gene therapy of primary myopathies. J Clin Invest 1998;101:2119–28.
[11] Goudenege S, Pisani DF, Wdziekonski B, Di Santo JP, Bagnis C, Dani C, et al. Enhancement of myogenic and muscle repair capacities of human adipose-derived stem cells with forced expression of MyoD. Mol Ther 2009;17:1064–72.
[12] Cooper ST, Kizana E, Yates JD, Lo HP, Yang N, Wu ZH, et al. Dystrophinopathy carrier determination and detection of protein deficiencies in muscular dystrophy using lentiviral MyoD-forced myogenesis. Neuromuscul Disord 2007;17:276–84.
[13] Itoh M, Yasunishi A, Imamura K, Kanamori-Katayama M, Suzuki H, Suzuki M, et al. Constructing ORFeome resources with removable termination codons. Biotechniques 2006;41:44,46,48.
[14] Kimura K, Wakamatsu A, Suzuki Y, Ota T, Nishikawa T, Yamashita R, et al. Diversification of transcriptional modulation: large-scale identification and characterization of putative alternative promoters of human genes. Genome Res 2006;16:55–65.
[15] Ota T, Suzuki Y, Nishikawa T, Otsuki T, Sugiyama T, Irie R, et al. Complete sequencing and characterization of 21,243 full-length human cDNAs. Nat Genet 2004;36:40–5.
[16] Otsuki T, Ota T, Nishikawa T, Hayashi K, Suzuki Y, Yamamoto J, et al. Signal sequence and keyword trap in silico for selection of full-length human cDNAs encoding secretion or membrane proteins from oligo-capped cDNA libraries. DNA Res 2005;12:117–26.
[17] Godmann M, May E, Kimmins S. Epigenetic mechanisms regulate stem cell expressed genes Pou5f1 and Gfra1 in a male germ cell line. PLoS One 2010;5:e12727.
[18] Nabeshima Y, Hanaoka K, Hayasaka M, Esumi E, Li S, Nonaka I. Myogenin gene disruption results in perinatal lethality because of severe muscle defect. Nature 1993;364:532–5.
[19] Rudnicki MA, Schnegelsberg PN, Stead RH, Braun T, Arnold HH, Jaenisch R. MyoD or Myf-5 is required for the formation of skeletal muscle. Cell 1993;75:1351–9.
[20] Parker MH, Seale P, Rudnicki MA. Looking back to the embryo: defining transcriptional networks in adult myogenesis. Nat Rev Genet 2003;4:497–507.
[21] Rudnicki MA, Le Grand F, McKinnell I, Kuang S. The molecular regulation of muscle stem cell function. Cold Spring Harb Symp Quant Biol 2008;73:323–31.
[22] Chargé SB, Rudnicki MA. Cellular and molecular regulation of muscle regeneration. Physiol Rev 2004;84:209–38.
[23] Kawamichi Y, Cui CH, Toyoda M, Makino H, Horie A, Takahashi Y, et al. Cells of extraembryonic mesodermal origin confer human dystrophin in the mdx model of Duchenne muscular dystrophy. J Cell Physiol 2010;223:695–702.
[24] González-Ramírez R, Morales-Lázaro SL, Tapia-Ramírez V, Mornet D, Cisneros B. Nuclear and nuclear envelope localization of dystrophin Dp71 and dystrophin-associated proteins (DAPs) in the C2C12 muscle cells: DAPs nuclear localization is modulated during myogenesis. J Cell Biochem 2008;105:735–45.
[25] Bujang-Safawi E, Halim AS, Khoo TL, Dorai AA. Dried irradiated human amniotic membrane as a biological dressing for facial burns – a 7-year case series. Burns 2010;36:876–82.
[26] Kolli S, Ahmad S, Lako M, Figueiredo F. Successful clinical implementation of corneal epithelial stem cell therapy for treatment of unilateral limbal stem cell deficiency. Stem Cells 2010;28:597–610.
[27] Mermet I, Pottier N, Sainthillier JM, Malugani C, Cairey-Remonnay S, Maddens S, et al. Use of amniotic membrane transplantation in the treatment of venous leg ulcers. Wound Repair Regen 2007;15:459–64.
[28] Cargnoni A, Gibelli L, Tosini A, Signoroni PB, Nassuato C, Arienti D, et al. Transplantation of allogeneic and xenogeneic placenta-derived cells reduces bleomycin-induced lung fibrosis. Cell Transplant 2009;18:405–22.
[29] Chen Z, Tortella FC, Dave JR, Marshall VS, Clarke DL, Sing G, et al. Human amnion-derived multipotent progenitor cell treatment alleviates traumatic brain injury-induced axonal degeneration. J Neurotrauma 2009;26:1987–97.
[30] Dekaris I, Gabrić N. Preparation and preservation of amniotic membrane. Dev Ophthalmol 2009;43:97–104.
[31] Toda A, Okabe M, Yoshida T, Nikaido T. The potential of amniotic membrane/amnion-derived cells for regeneration of various tissues. J Pharmacol Sci 2007;105:215–28.

Case Report

Acta Hæmatologica

Acta Haematol 2013;129:238–242
DOI: 10.1159/000345727

Received: September 27, 2012
Accepted after revision: October 29, 2012
Published online: January 12, 2013

Acute Leukemia Showing t(8;22)(p11;q11), Myelodysplasia, CD13/CD33/CD19 Expression and Immunoglobulin Heavy Chain Gene Rearrangement

Masaya Shimanuki Takashi Sonoki Hiroki Hosoi Jyuri Watanuki
Shogo Murata Toshiki Mushino Kodai Kuriyama Shinobu Tamura
Kazuo Hatanaka Nobuyoshi Hanaoka Hideki Nakakuma

Hematology/Oncology, Wakayama Medical University, Wakayama, Japan

Key Words
Acute leukemia · Myeloid/B-lymphoid disorder · t(8;22)(p11;q11)

Abstract
t(8;22)(p11;q11) is a rare but recurrent chromosome translocation that has been reported in 11 cases of myeloproliferative neoplasm or B-acute lymphoblastic leukemia. This translocation results in an in-frame fusion of *FGFR1* on 8p11 and *BCR* on 22q11, and causes constitutive activation of the tyrosine kinase of the BCR/FGFR1 chimera protein. Here, we report the twelfth case of hematological tumor bearing t(8;22)(p11;q11). The bone marrow showed hypoplastic and tri-lineage dysplasia with 24.4% abnormal cells. The abnormal cells were not defined as myeloid or lymphoid morphologically, lacking a myeloperoxidase reaction. Flow cytometric analysis of the bone marrow cells revealed that the abnormal cells expressed CD13, CD33, CD34, and CD19, and that a fraction of the abnormal cells was positive for CD10. Southern blot analysis of the bone marrow cells showed rearrangement of the immunoglobulin heavy chain gene, a genetic hallmark of B-cell differentiation. Previously reported cases with t(8;22)(p11;q11) suggested an association between myeloid and B-lymphoid tumors, whereas other chromosome translocations involving *FGFR1* on 8p11 showed a link between myeloid and T-lymphoid tumors. Our observation supports that t(8;22)(p11;q11) might define a dual myeloid and B-lymphoid disorder.

Introduction

t(8;22)(p11;q11) is a rare but recurrent genetic alteration that has been reported in 11 patients with hematological malignancies, including 9 with myeloproliferative neoplasm (MPN) [1–7, 10] and 2 with B-cell acute lymphoblastic leukemia (B-ALL) [8, 9]. This translocation results in a fusion between the fibroblast growth factor receptor 1 gene *(FGFR1)* on 8p11 and the breakpoint cluster region gene *(BCR)* on 22q11. As a consequence of this translocation, the tyrosine kinase of the chimeric BCR/FGFR1 is constitutively activated [2, 11], similar to ABL

KARGER

Fax +41 61 306 12 34
E-Mail karger@karger.com
www.karger.com

0001–5792/13/1294–0238$38.00/0

Accessible online at:
www.karger.com/aha

Takashi Sonoki, MD, PhD
Hematology/Oncology, Wakayama Medical University
Kimiidera 811-1
Wakayama 641-8509 (Japan)
E-Mail sonoki@wakayama-med.ac.jp

kinase activity in BCR/ABL chimera. Animal models mimicking t(8;22)(p11;q11) developed MPN [11, 12] and B-ALL [13], indicating that t(8;22)(p11;q11) plays a crucial role in tumorigenesis and that this translocation can cause tumors of myeloid and B-lymphoid cells. Interestingly, previously reported MPN with t(8;22)(p11;q11) exhibited unusual B-cell proliferation even in the chronic phase [1, 2, 10]. In addition, two B-ALL patients showed curious proliferation of myeloid cells after remission of B-ALL [8, 9]. These experimental and clinical results suggested that t(8;22)(p11;q11) might define a dual myeloid and B-lymphoid proliferative disorder [4, 13].

Here, we report the twelfth case of hematological malignancy with t(8;22)(p11;q11). The tumor cells of this patient showed some features compatible with a dual myeloid and B-lymphoid disorder. Firstly, the bone marrow cells showed multi-lineage dysplasia, suggesting impaired myeloid differentiation. Secondly, the tumor cells harbored concurrently myeloid and B-lymphoid lineage markers. Finally, the bone marrow cells showed clonal rearrangements of the immunoglobulin heavy chain gene *(IGH)*, although no apparent B-lymphoid tumor was seen in the bone marrow. Our results support that the tumor cells exhibiting t(8;22)(p11;q11) represent a dual myeloid and B-lymphoid disorder, as proposed in previous reports [4, 13].

Case Report

A 58-year-old woman, with no history of hematological disease, was admitted because of general fatigue. On examination, there was no hepatosplenomegaly. Her WBC was 1.5×10^9/l with 1% abnormal cells, 1% metamyelocytes, 32% neutrophils, 62% lymphocytes, no eosinophils or basophils, macrocytic anemia of Hb 10.0 g/dl, and platelet count 85×10^9/l. Bone marrow smear revealed hypoplastic marrow. There were 30×10^9/l total nucleated cells, consisting of 5.6% myelocytes, 7.2% metamyelocytes, 26.8% granulocytes, 0.8% monocytes, 1.6% erythroblasts, 0.4% histiocytes, 33.2% lymphocytes, and 24.4% abnormal cells. The abnormal cells were morphologically not defined as myeloid or lymphoid (fig. 1A) and were negative for a myeloperoxidase reaction. In addition to increased abnormal cells, dysplasia of multilineage cells was found (fig. 1A). The abnormal cells were concurrently positive for myeloid and B-lymphoid lineage markers (CD13 and CD19, respectively) (fig. 1B). In addition, the abnormal cells were positive for CD33 and CD34, and some fraction of these was positive for CD10 (fig. 1B). On the basis of these findings, the patient was diagnosed with de novo acute leukemia with multilineage dysplasia. Conventional G-banding analysis of the bone marrow cells showed 45,XX,t(8;22)(p11;q11),-16,add(19)(p13) in 16 out of 20 metaphases. Chimera transcripts of *BCR/ABL*, *TEL/AML1*, *E2A/PBX1*, *CBFβ/MYH11*, *MLL/AF4* and *MLL/AF9* were all negative. This patient was treated with chemotherapy with a CAG regimen (cytarabine 10 mg/m^2 subcutaneously every 12 h for 14 days; aclarubicin hydrochloride 10 mg/m^2 per day, drip injection for 4 days, and granulocyte colony-stimulating factor 100 μg/day, subcutaneous injection for 14 days) for 3 courses, but leukemic cells were retained in peripheral blood. Subsequently, she received an allogeneic peripheral blood stem cell transplantation from an HLA-identical sibling; however, the patient died due to disease recurrence 8 months after the initial diagnosis. G-banding analysis of bone marrow cells at relapse was 45,X,-X,t(8;22)(p11;q11),-16,-17,-18,add(19)(p13).

Materials and Methods

RT-PCR, Sequence Analysis, and Southern Blot Analysis

RT-PCR was performed using the PrimeScript One Step RT-PCR Kit Ver.2 (Takara, Kyoto, Japan). A *BCR/FGR1* chimeric transcript was amplified using specific primers for *BCR* exon 1 (E1+ primer) and *FGFR1* exon 9 (FGFR9-primer), as described by Demiroglu et al. [2]. The reciprocal fusion transcript *FGFR1/BCR* was amplified using primer pairs set at *FGFR1* exon 7 and *BCR* exon 8 according to a previous report by Fioretos et al. [1]. The nucleotide alignments of the PCR products were determined directly and analyzed through the BLAST search program.

For Southern blot analysis, high molecular DNA was digested with Bgl II, Hind III, or Pst I. The digested DNA was transferred onto a nylon membrane (Roche, Mannheim, Germany). A Hinc II fragment of 1.0 kb containing the human *IGH* joining was used as a probe. Hybridization and washing were performed as previously described [14].

Results

Both *BCR/FGFR1* chimera and its reciprocal chimera *FGFR1/BCR* were detected by RT-PCR (fig. 1C). The *BCR/FGFR1* chimera showed an in-frame fusion of *BCR* exon 4 and *FGFR1* exon 9 as determined by sequence analysis (accession No. AB742170). The *FGFR1/BCR* product was confirmed as an in-frame recombination of *FGFR1* exon 8 with *BCR* exon 5 (accession No. AB742171). Since the tumor cells expressed CD19 as well as myeloid lineage markers, we next performed Southern blot analysis using the *IGH* joining region probe. As illustrated in figure 1D, the bone marrow cells showed *IGH* rearrangement by various enzyme digestions.

Discussion

t(8;22)(p11;q11) was originally found in patients diagnosed with atypical chronic myeloid leukemia lacking t(9;22)(q34;q11) [1, 2]. Subsequently, this translocation was found in B-ALL patients. To date, 11 cases with t(8;

Acta Haematol 2013;129:238–242
DOI: 10.1159/000345727

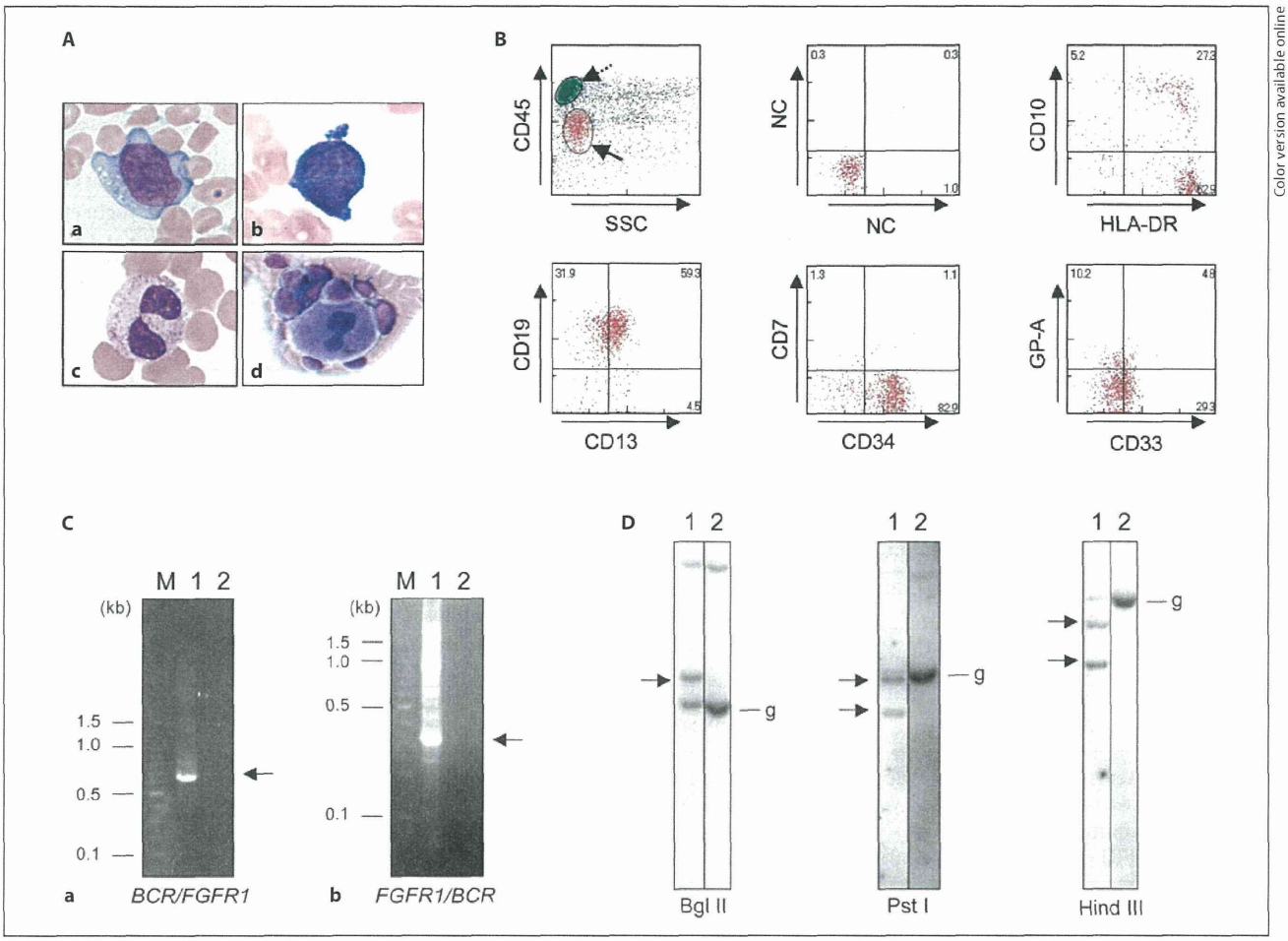

Fig. 1.A Morphological aspects of abnormal cells seen in the bone marrow. Leukemic cell (a), erythroid cell with 2 nuclei (b), granulocyte with a pseudo-Pelger anomaly (c), and hypo-segmented megakaryocyte (d). **B** Phenotypic aspects of bone marrow cells by flow cytometric analysis. $CD45^{int}$ and SSC^{low} cells (solid arrow), which represented leukemic cells, were further analyzed for lineage markers. The leukemic cells were positive for CD13, CD33, CD34, and CD19. A fraction of the leukemic cells was positive for CD10. Lineage marker analysis of the cells indicated by dotted arrow revealed that the population was composed of 86.2% $CD3^+$, 44.0% $CD4^+$, 40.4% $CD8^+$, 13.4% $CD56^+$, 0.6% $CD10^+$, 6.6% $CD19^+$, 8.7% $CD20^+$, 2.1% $CD13^+$ and 1.5% $CD33^+$ cells. **C** RT-PCR of *BCR/FGFR1* and *FGFR1/BCR* chimera transcripts. Lane M: 100-bp DNA marker (Takara, Kyoto, Japan), lane 1: patient, lane 2: negative control. Arrows indicate chimera transcripts. Numbers on the left side of the pictures indicate DNA size. The nucleotide alignments of both products were registered in the EMBL/Genbank/DDJB database (AB742170 and AB742171). **D** Southern blot analysis of the *IGH* joining region. The bone marrow cells showed rearrangements (arrows). Lane 1: patient's bone marrow cells, lane 2: germ line control. g = Germ-line band.

22)(p11;q11) have been reported, consisting of 9 with MPN and2 with B-ALL (table 1). Other chromosome translocations involving *FGFR1* on 8p11, such as t(8;13)(p11;q12), are associated with eosinophilia and T-cell lymphoblastic lymphoma, called 8p11 myeloproliferative syndrome (EMS, 8 p11 myeloproliferative syndrome) [15]. In contrast, t(8;22)(p11;q11) does not seem to be associated with these phenotypes, although 1 MPN case developed T-lymphoblastic lymphoma concurrently [10]. In reviewing the literature, it appeared that t(8;22)(p11;q11) might have a link with aberrant proliferation of both myeloid and B-lymphoid cells. Among the 9 MPN with t(8;22)(p11;q11)-positive patients, 4 showed aberrant lymphoid proliferation at the initial diagnosis in the chronic

Table 1. Characteristics of 12 patients with t(8;22)(p11;q11)

No.	Age/Sex	Diagnosis	Transformation	Myeloblasts or blasts	B-lymphoid	[Ref.]
1	75/M	MPN	AML	9% of blasts (MPO–)	Proliferation of polyclonal B-lymphocytes at diagnosis	Fioretos et al. [1]
2	65/F	MPN	None	4% of myeloblasts	ND	Demiroglu et al. [2]
3	51/F	MPN	None	4% of myeloblasts	4% of B-lymphoblasts	Demiroglu et al. [2]
4	74/F	MPN	None	3% of blasts	ND	Pini et al. [3]
5	68/F	MPN	B-lymphoid crisis	ND	5% of lymphoblasts[b] at diagnosis 22% of B-lymphoblasts at crisis (CD13+)	Murati et al. [4]
6[a]	58/F	MPN	AML	ND	ND	Agerstam et al. [5]
7[a]	50/F	MPN (AP)	Blastic crisis	1% of myeloblasts	ND	Lee et al. [6]
8	56/F	MPN	AML (FAB; M0)	54% of myeloblasts at crisis (MPO–/CD19+)	ND	Richebourg et al. [7]
9	70/F	B-ALL	Thrombocytosis and granulocytosis with dysplasia	ND	B-lymphoblasts at diagnosis	Baldazzi et al. [8]
10	43/M	B-ALL	CML-like disease	ND	84% of B-lymphoblasts at diagnosis	Wakim et al. [9]
11	59/M	MPN T-LBL	None	15% of myeloblasts	Proliferation of B-lymphocytes in BM at diagnosis	Kim et al. [10]
12	58/F	AL with dysplasia	None	24.4% of blasts (MPO–/CD10+/CD19+)	IGHJ rearrangement at diagnosis	Present case

B-ALL = Acute B-cell lymphoblastic leukemia; T-LBL = T-cell lymphoblastic lymphoma; AL = acute leukemia; AML = acute myelogenous leukemia; CML = chronic myelogenous leukemia; MPO = myeloperoxidase; ND = not described; IGHJ = immunoglobulin heavy chain joining region.

[a] *BCR/FGFR1* chimera was not confirmed in these patients. [b] Cell surface antigens were not examined.

phase (No. 1, 3, 5, and 11 in table 1). In patients 1, 3, and 11, the lymphoid cells were defined as B-cells [1, 2, 10]. In patient 5, increase in immature lymphocytes was seen in the bone marrow at the initial diagnosis, but the phenotype was not examined; however, leukemic cells in blastic crisis were defined as B lymphoblasts, suggesting that immature lymphocytes at the initial diagnosis would be B-cells [4]. Even in the 2 B-ALL patients (No. 9 and 10 in table 1), their clinical courses suggested the involvement not only of B-lymphoid but also of myeloid cells. Patients 9 and 10 showed unusual thrombocytosis/granulocytosis and CML-like disease after remission of B-ALL, respectively [8, 9]. The phenotypes of the leukemic cells of patients (No. 5 and 8 and the present case 12 in table 1) were also notable. The 3 leukemic cells were positive for myeloid and B-lymphoid markers, suggesting that leukemic cells exhibited a dual myeloid and B-lymphoid phenotype. Although Southern blot analysis was performed in patient 3, there was no detectable *IGH* rearrangement [2]. We demonstrated *IGH* rearrangements in peculiar leukemic cells showing t(8;22)(p11;q11) and myeloid and B-lymphoid lineage markers, indicating that the leukemic cells might belong to the B-cell lineage genetically. Recently, the existence of myeloid/B-lymphoid progenitor (MBP) cells that can generate both myeloid and B-lymphoid cells has been proposed [16]. Murati et al. [4] discussed that t(8;22)(p11;q11)-positive tumor cells could originate from MBP, and that t(8;22)(p11;q11) might define dual myeloid and B-lymphoid disorder. Our present observations support that t(8;22)(p11;q11)-positive tumor cells represent a myeloid and B-lymphoid disorder, which might be distinguished from other hematological malignancies with 8p11 rearrangements showing dual myeloid and T-lymphoid disorder.

References

1 Fioretos T, Panagopoulos I, Lassen C, Swedin A, Billström R, Isaksson M, Strömbeck B, Olofsson T, Mitelman F, Johansson B: Fusion of the BCR and the fibroblast growth factor receptor-1 (FGFR1) genes as a result of t(8;22)(p11;q11) in a myeloproliferative disorder: the first fusion gene involving BCR but not ABL. Genes Chromosomes Cancer 2001;32:302–310.

2 Demiroglu A, Steer EJ, Heath C, Taylor K, Bentley M, Allen SL, Koduru P, Brody JP, Hawson G, Rodwell R, Doody ML, Carnicero F, Reiter A, Goldman JM, Melo JV, Cross NC: The t(8;22) in chronic myeloid leukemia fuses BCR to FGFR1: transforming activity and specific inhibition of FGFR1 fusion proteins. Blood 2001;98:3778–3783.

3 Pini M, Gottardi E, Scaravaglio P, Giugliano E, Libener R, Baraldi A, Muzio A, Cornaglia E, Saglio G, Levis A: A fourth case of BCR-FGFR1 positive CML-like disease with t(8;22) translocation showing an extensive deletion on the derivative chromosome 8p. Hematol J 2002;3:315–316.

4 Murati A, Arnoulet C, Lafage-Pochitaloff M, Adélaide J, Derré M, Slama B, Delaval B, Popovici C, Vey N, Xerri L, Mozziconacci MJ, Boulat O, Sainty D, Birnbaum D, Chaffanet M: Dual lympho-myeloproliferative disorder in a patient with t(8;22) with BCR-FGFR1 gene fusion. Int J Oncol 2005;26:1485–1492.

5 Agerstam H, Lilljebjörn H, Lassen C, Swedin A, Richter J, Vandenberghe P, Johansson B, Fioretos T: Fusion gene-mediated truncation of RUNX1 as a potential mechanism underlying disease progression in the 8p11 myeloproliferative syndrome. Genes Chromosomes Cancer 2007;46:635–643.

6 Lee SG, Park TS, Lee ST, Lee KA, Song J, Kim J, Suh B, Choi JR, Park R: Rare translocations involving chromosome band 8p11 in myeloid neoplasms. Cancer Genet Cytogenet 2008;186:127–129.

7 Richebourg S, Theisen O, Plantier I, Parry A, Soenen-Cornu V, Lepelley P, Preudhomme C, Renneville A, Laï JL, Roche-Lestienne C: Chronic myeloproliferative disorder with t(8;22)(p11;q11) can mime clonal cytogenetic evolution of authentic chronic myelogeneous leukemia. Genes Chromosomes Cancer 2008;47:915–918.

8 Baldazzi C, Iacobucci I, Luatti S, Ottaviani E, Marzocchi G, Paolini S, Stacchini M, Papayannidis C, Gamberini C, Martinelli G, Baccarani M, Testoni N: B-cell acute lymphoblastic leukemia as evolution of a 8p11 myeloproliferative syndrome with t(8;22)(p11;q11) and BCR-FGFR1 fusion gene. Leuk Res 2010;34:e282–e285.

9 Wakim JJ, Tirado CA, Chen W, Collins R: t(8;22)/BCR-FGFR1 myeloproliferative disorder presenting as B-acute lymphoblastic leukemia: report of a case treated with sorafenib and review of the literature. Leuk Res 2010;35:e151–e153.

10 Kim SY, Oh B, She CJ, Kim HK, Jeon YK, Shin MG, Yoon SS, Lee DS: 8p11 myeloproliferative syndrome with BCR-FGFR1 rearrangement presenting with T-lymphoblastic lymphoma and bone marrow stromal cell proliferation: a case report and review of the literature. Leuk Res 2011;35:e30–e34.

11 Roumiantsev S, Krause DS, Neumann CA, Dimitri CA, Asiedu F, Cross NC, Van Etten RA: Distinct stem cell myeloproliferative/T lymphoma syndromes induced by ZNF198-FGFR1 and BCR-FGFR1 fusion genes from 8p11 translocations. Cancer Cell 2004;5:287–298.

12 Agerstam H, Järås M, Andersson A, Johnels P, Hansen N, Lassen C, Rissler M, Gisselsson D, Olofsson T, Richter J, Fan X, Ehinger M, Fioretos T: Modeling the human 8p11-myeloproliferative syndrome in immunodeficient mice. Blood 2010;116:2103–2111.

13 Ren M, Tidwell JA, Sharma S, Cowell JK: Acute progression of BCR-FGFR1 induced murine B-lympho/myeloproliferative disorder suggests involvement of lineages at the pro-B cell stage. PLoS One 2012;7:e38265.

14 Watanuki J, Hatakeyama K, Sonoki T, Tatetsu H, Yoshida K, Fujii S, Mizutani M, Abo T, Kurimoto M, Matsuoka H, Matsuno F, Nakakuma H: Bone marrow large B cell lymphoma bearing cyclin D3 expression: clinical, morphologic, immunophenotypic, and genotypic analyses of seven patients. Int J Hematol 2009;90:217–225.

15 Macdonald D, Reiter A, Cross NC: The 8p11 myeloproliferative syndrome: a distinct clinical entity caused by constitutive activation of FGFR1. Acta Haematol 2002;107:101–107.

16 Kawamoto H, Katsura Y: A new paradigm for hematopoietic cell lineages: revision of the classical concept of the myeloid-lymphoid dichotomy. Trends Immunol 2009;30:193–200.

European Journal of Haematology

European Journal of Haematology 90 (59–67)

ORIGINAL ARTICLE

Molecular cloning of *IGλ* rearrangements using long-distance inverse PCR (LDI-PCR)

Masaya Shimanuki[1], Takashi Sonoki[1], Hiroki Hosoi[1], Jyuri Watanuki[1], Shogo Murata[1], Keiki Kawakami[2], Hiroshi Matsuoka[1,3], Nobuyoshi Hanaoka[1], Hideki Nakakuma[1]

[1]Hematology/Oncology, Wakayama Medical University, Wakayama; [2]Division of Hematology, Suzuka General Hospital, Suzuka; [3]Department of Oncology and Hematology, Kobe University School of Medicine, Kobe, Japan

Abstract

Objectives: Malignant cells of mature B-cell origin show tumor-specific clonal immunoglobulin gene (*IG*) rearrangements, including *V(D)J* recombinations, nucleotide mutations, or translocations. Rapid molecular cloning of the breakpoint sequence by long-distance inverse PCR (LDI-PCR) has so far been applied to rearrangements targeted to *IGH* joining, *IGH* switch, and *IGκ* regions. We tended to apply LDI-PCR method for cloning of *IGλ* rearrangements. *Methods:* To identify which *IGλ* isotype segment was rearranged, we performed Southern blot analysis using isotype-specific probes. We set inverse primers on the telomeric side of each joining region and amplified rearranged bands detected by Southern blot analysis as corresponding PCR products. *Results:* All germline *IGλ* segments were successfully amplified as expected PCR products. We determined breakpoint sequences of five chromosome translocations involving *IGλ* locus: three novel t(8;22)(q24;q11), one known t(3;22)(q27;q11), and one partially known t (11;22)(q13;q11). Two of the three t(8;22)(q24;q11) were involved in *Jλ* with a recombination signal sequence and one of three in the first exon of *IGLL5*, which lies upstream of *Jλ1*. Three 8q24 breakpoints were widespread at 132, 260 and 366 kb downstream of *MYC* locus. The t(3;22)(q27;q11) showed a juxtaposition of *Jλ2* and the first intron of *BCL6*, as previously reported. In t(11;22)(q13;q11), 3′UTR of *cyclin D1* fused to the constant region of *λ7* with nucleotide mutations. We also amplified four *Vλ/Jλ* recombination sequences. *Conclusion:* Our method is a useful tool for molecular analysis of genetic events in *IGλ*.

Key words *IGλ*; rearrangements; translocation; molecular cloning; LDI-PCR

Correspondence Takashi Sonoki, MD, PhD, Hematology/Oncology, Wakayama Medical University, Kimi-idera 811-1, Wakayama 641-8510, Japan. Tel: +81 73 441 0665; Fax: +81 73 441 0653; e-mail: sonoki@wakayama-med.ac.jp

Accepted for publication 26 October 2012

doi:10.1111/ejh.12037

Malignant tumor cells of mature B-cell origin show tumor-specific rearrangements of immunoglobulin genes (heavy chain gene, *IGH*; kappa light chain gene, *IGκ*; and lambda light chain gene, *IGλ*). The vast majority of the tumor cells have functional *IG* rearrangements, *V(D)J* recombinations, for synthesis of IG protein, and most exhibit chromosome translocations targeted to *IG* loci (*IGH* on 14q32, *IGκ* on 2p12, and *IGλ* on 22q11). In the case of chromosome translocations, molecular cloning of the translocation breakpoints identified many oncogenes that play crucial roles in the pathogenesis of B-cell tumors (1). The consequence of the translocations is close apposition of partner genes into putative *IG* transcription elements, resulting in deregulated expression of the affected genes. On the other hand, determination of the nucleotide alignment of functional *IG* gene rearrangements or chromosome translocations in B-cell tumors helps us to understand the tumor cell origin, because *IG* genes undergo genetic modifications in an ordered manner during B-cell maturation steps, such as *V(D)J* recombinations mediated by recombination activating gene 1 and 2 products (RAG1/2) at an early stage of differentiation in bone marrow or somatic hypermutation (SHM) within the variable region and *IGH* class switch recombination, both

mediated by activation-induced cytidine deaminase (AID), at the late stage of differentiation in lymph nodes (2, 3).

Inverse PCR is a method for identifying unknown sequences by primer set on the known flanking nucleotide sequence in opposite orientation using self-ligated circular DNAs as PCR templates. The combination of this method and long-distance thermostable DNA polymerase, namely long-distance inverse PCR (LDI-PCR), was first applied for rapid molecular cloning of *IGH*-joining (*IGHJ*) rearrangements (4). Subsequently, LDI-PCR was applied for *IGH* switch (*IGHS*) translocations and recently *IGκ* translocations (5, 6), but not yet for *IGλ* locus. LDI-PCR requires a small amount of material and a couple of days for molecular cloning; therefore, this method allows us to analyze genetic events of *IG* genes easily.

Here, we report the application of LDI-PCR for molecular cloning of rearrangements targeted to the *IGλ* gene locus. Using this method, we identified breakpoint sequences of five chromosome translocations, including three novel t(8;22)(q24;q11), one known t(3;22)(q27;q11), and one partially known t(11;22)(q13;q11) as well as four *VλJλ* recombination sequences.

Materials and methods

Cell lines and patients

Four cell lines (MD901, WILL2, KHM10B, and KHM2B) and two clinical samples (patient 1 and 2) were analyzed in this study. MD901 was derived from a patient with diffuse large B-cell lymphoma (DLBCL) (a kind gift from Dr. T. Miki at Tokyo Medical and Dental University, Japan) (7). The cell was reported to be positive for cell surface IGκ and showed t(3;22)(q27;q11) and t(8;22)(q24;q11) cytogenetically. The t(3;22)(q27;q11) has been identified as a fusion of the first intron of *BCL6* and *Jλ2* (7). WILL2 was established from a patient with DLBCL showing surface IGλ and t(8;22)(q24;q11) in our laboratory (8). KHM10B and KHM2B were established from patients diagnosed with B-cell type of acute lymphoblastic leukemia (FAB: L3) (purchased from JCRB, Osaka, Japan) (9, 10). Both KHM10B and KHM2B are positive for surface IGλ. KHM10B has a t(8;22)(q24;q11), and KHM2B has a t(8;14)(q24;q32) and a t(14;18)(q32;q21). Patient 1 was diagnosed with malignant lymphoma, morphologically not otherwise specified (11). The tumor cells of this patient were positive for IGκ on the cell surface and exhibited multiple *IG* translocations: t(14;18)(q32;q21), t(3;14)(q27;q32), t(8;14)(q24;q32), and t(11;22)(q13;q32). Partial nucleotide alignments of t(11;22)(q13;q11) were described elsewhere (11). Patient 2 was diagnosed with DLBCL-bearing surface IGλ, and the tumor cells were shown to have t(6;14)(p21;q32) (12). Table 1 summarizes the characteristics of the cell lines and the patients analyzed in this work.

Table 1 Characteristics of cell lines and patients

Cell	Disease entity	*IG* translocations	Surface IG light chain
MD901	DLBCL	t(3;22)(q27;q11) t(8;22)(q24;q11)	Kappa
WILL2	DLBCL	t(14;18)(q32;q21) t(8;22)(q24;q11)	Lambda
KHM10B	ALL (FAB; L3)	t(8;22)(q24;q11)	Lambda
KHM2B	ALL (FAB; L3)	t(14;18)(q32;q21) t(8;14)(q24;q32)	Lambda
Patient 1	Mature B-cell lymphoma (not otherwise specified)	t(3;14)(q27;q32) t(8;14)(q24;q32) t(14;18)(q32;q21) t(11;22)(q13;q11)	Kappa
Patient 2	DLBCL	t(6;14)(p21;q32)	Lambda

DLBCL, diffuse large B-cell lymphoma; ALL, acute lymphoblastic leukemia.

Southern blot analysis

Eight DNA fragments (IGLC1D, IGLJ2, IGLC2D, IGLC3, IGLC4D, IGLJ5, IGLJ6, and IGLJ7) were used as probes to define which isotype was rearranged (13, 14). IGLC1D, IGLC2D, IGLC4D, IGLJ5, IGLJ6, and IGLJ7 are specific for λ1, λ2, λ4, λ5, λ6, and λ7 segments, respectively (14). IGLJ2 recognizes λ2 and λ3 regions, and IGLC3 can hybridize to all λ segments (13, 14). All DNA fragments were labeled with digoxigenin using a PCR DIG Probe Synthesis kit (Roche, Mannheim, Germany). Southern blot analysis was performed according to the manufacturer's recommendations. An enzyme map of the *IGλ* and probe positions, except IGLC3, is shown in Fig. S1A.

LDI-PCR for *IGλ* locus

In chromosome translocation involving the *IGλ* locus, the telomeric end of 22q11 moves to the translocation partner chromosome and affects the expression of the responsible gene located on the partner chromosome as shown in Fig. S1. Thus, we set all primers on the telomeric sides of each *IGλ* isotype segment. The primers used in this work are listed in Table S1, and the positions are illustrated in Fig. S1. The size of the PCR product of interest was expected to be smaller than the rearranged bands seen in Southern blot analysis owing to the physical distance of forward and reverse primers (Table S2).

A 50 μL of reaction mix included an aliquot of circular DNA, 5 μL of 10× LA PCR BufferII, 2.5 mM $MgCI_2$, 2.5 mM dNTP mixture, 10% vol. of DMSO, and two units of LA-Taq polymerase (LA-Taq; TaKaRa, Kyoto, Japan). The 1st and 2nd round PCRs were run at 25 and 30 cycles, respectively. All germline segments of *IGλ* isotype can be amplified as shown in Fig. S1. The PCR products of interest were isolated by a gel extraction kit (Qiagen, Hilden, Germany) and then subjected to sequence analysis directly or

after subcloning into pGEM/T easy vector (Promega, Madison, WI, USA).

Verification of LDI-PCR and analysis of breakpoint sequences

To confirm the reliability of the LDI-PCR result, we set specific primers at each breakpoint of translocation or functional recombinations based on the nucleotide alignments obtained by LDI-PCR. DNA fragments around the breakpoints were amplified using high-fidelity Taq polymerase (PrimeSTAR; TaKaRa, Kyoto, Japan) and the respective breakpoint-specific primers, which are listed in Table S3. The nucleotide alignments of the PCR products were determined directly by 'sequence walking' at a sequencing facility (Fasmac, Chiba, Japan).

Database analysis

All nucleotide alignments of PCR products were analyzed using the BLAST search program (15). The Human BLAT Search program (http://genome.ucsc.edu/) was used to map the 8q24 breakpoint sequences onto chromosomes 8 (16). According to the human genome build hg19 primary assembly, *MYC* and *PVT1* are mapped from Chr. 8. 128 747 765 to 128 751 018 nt and from Chr. 8. 128 806 779 to 129 113 499 nt, respectively. Cryptic recombination signal sequences were searched by RSSsite (www.itb.cnr.it/rss/analyze/) (17). Four *Vλ/Jλ* sequences were analyzed using IgBLAST (www.ncbi.nlm.nih.gov/igblast/). Partial nucleotide alignments of breakpoints cloned from translocations or *Vλ/Jλ* recombinations in this study have been deposited in the EMBL/Genbank/DDJB database (accession no. AB720049-AB720052 for translocations and AB724295-AB724298 for *Vλ/Jλ* recombinations).

Results

Molecular cloning of chromosome translocation break points involving *IGλ* locus

MD901 cells show biallelic 22q11 translocations, t(3;22)(q27;q11) and t(8;22)(q24;q11). The breakpoint of t(3;22)(q24;q11) has been cloned, but that of the t(8;22)(q24;q11) remains unclear (7). We searched for *IGλ* rearrangements by Southern blot analysis using isotype-specific probes and found a rearrangement by the IGLC1D probe. A 13.5 kb rearranged band of BglII digest was amplified by LDI-PCR using the lambda 1 primer set as a 9.9 kb PCR product (Fig. 1A). The 22q11 was truncated in the first exon of *IGLL5* (immunoglobulin lambda like 5) and fused to 8q24 at Chr. 8. 129 117 075 nt according to the human genome build hg19 assembly. The 8q24 breakpoint is 366 kb downstream from the *MYC* locus (Fig. 2A). The breakpoint sequence of t(3;22)(q27;q11) was also cloned. As shown in Fig. 1B, a 4.8 kb rearranged band detected with the IGLC3 probe on HindIII blot was amplified. Sequence analysis confirmed that the PCR product contained the same junction sequence between *Jλ2* and the first intron of *BCL6*, as in a previous report (data not shown) (7).

WILL2 cell line was established from a surface IGλ-positive DLBCL exhibiting t(8;22)(q24;q11) (8). Using the IGLJ2 probe, this cell showed two rearranged bands, suggesting that one represented a *Vλ/Jλ* recombination and another a translocation within the *λ2* or *λ3* segments (data not shown). Southern blot analysis of SphI digest probed with IGLC3 detected a 4.0-kb rearranged band, which was amplified using the lambda 2a primer set as a corresponding PCR product (Fig. 1C). Sequence analysis of the PCR product revealed that *Jλ2* fused to 129 010 874 nt on chromosome 8, which is 260 kb downstream from the *MYC* locus (Fig. 2A).

KHM10B has t(8;22)(q24;q11) and is positive for surface IGλ (9). Southern blot analysis showed two rearrangements in the *IGλ* locus, in *λ2* and *λ3* (data not shown). The 3.8 kb rearranged band seen in Taq I digest probed with IGLJ2 was amplified using the lambda 3a primer set as a 2.9 kb PCR product (Fig. 1D). Sequence analysis showed that *Jλ3* fused to 128 883 351 nt on chromosome 8, which is 132 kb downstream of *MYC* (Fig. 2A).

Patient 1 was reported to have t(11;22)(q13;q11) (11). In a previous study, the partial breakpoint sequence of t(11;22)(q13;q11) was determined using an inverse primers setting within *CCND1* on 11q13 (11). The sequence results suggested that 3′UTR of *CCND1* fused to *λ7* segment, but the precise breakpoint was not identified. The break point from 22q11 side was amplified using the lambda 7 primer set and EcoRI digest (Fig. 1E). Sequence analysis of the PCR product revealed that 3′UTR of *CCND1* fused to the constant region of *λ7*. The der(11) breakpoint fell to 16 369 nt of the *CCND1* sequence (accession no. NG_007375), which is 948 bp upstream of a previously reported der(11)t(11;22)(q13;q11) breakpoint (Fig. 2B) (18).

All translocation breakpoint sequences were verified as the expected sized DNA fragments by PCR using breakpoint-specific primers (Fig. 1F).

Analysis of nucleotide alignments around the translocation break points

To examine the nucleotide alignment around the break points further, the sequence of the PCR products, which were amplified using high-fidelity Taq polymerase and breakpoint-specific primers, was determined.

In MD901, 800 bp of the DNA sequence encompassing the der(8) breakpoint (accession no. AB720049) was determined. The 800-bp fragment consists of 227 and 573 bp

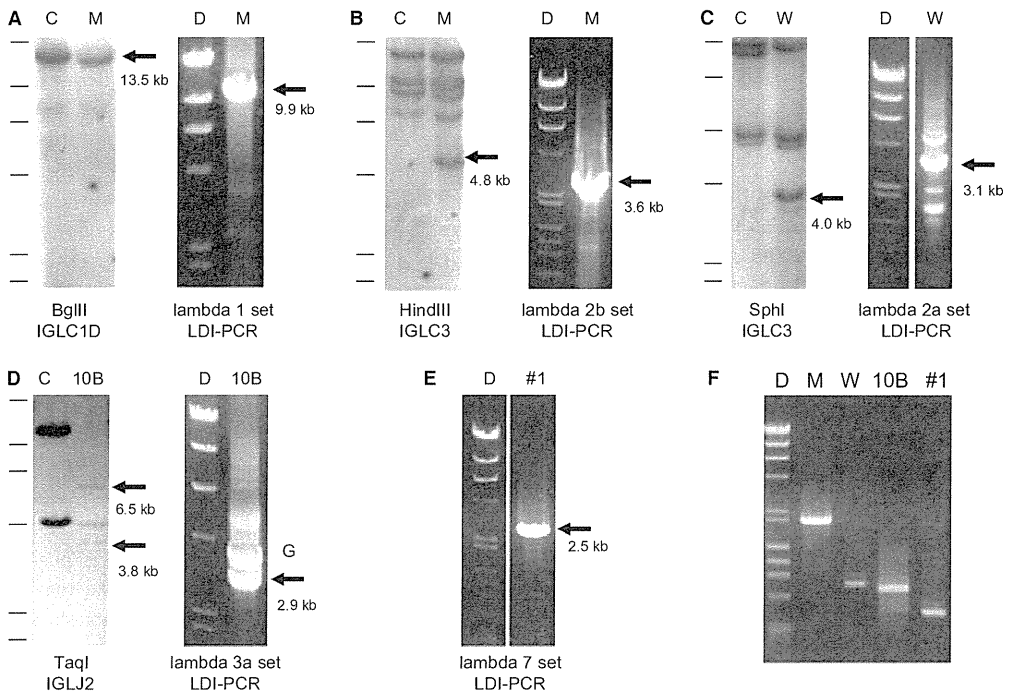

Figure 1 Molecular cloning of translocation breakpoints by LDI-PCR. (A) MD901 showed a rearrangement of λ1 locus. A 13.5-kb rearranged band (arrow) was amplified as a corresponding 9.9-kb PCR product (arrow). (B) MD901 showed a 4.8-kb rearranged band on HindIII digest (arrow) probed with IGLC3. The rearranged band was cloned by LDI-PCR (arrow). (C) WILL2 cells showed a 4.0-kb rearranged band on SphI blot probed with IGLC3 (arrow). The rearranged band was cloned by LDI-PCR (arrow). (D) KHM10B showed two rearranged bands on TaqI blot probed with the IGLJ2 (arrows). A 3.8-kb rearranged band (arrow) and a germline band (G) were amplified as corresponding DNA fragments by LDI-PCR. (E) Amplification of der(11)t(11;22)(q13;11) by LDI-PCR using lambda 7 set primers and EcoRI digest. (F) LDI-PCR results were verified for each sample using breakpoint-specific primer pairs. Expected sized DNA fragments were yielded by PCR (Table S3). M, W, 10B, #1, C, and D indicate MD901, WILL2, KHM10B, patient 1, germline control, and DNA marker (λ/Hind III and φ/Hae III digests), respectively.

derived from 8q24 and 22q11, respectively. The 227 bp of 8q24 showed no nucleotide mutation, but the 573 bp of 22q11 had two nucleotide substitutions (571/573; 99% match) against the germline *IGλ* reference sequence (accession no. NG_000002.1). Fig. 3A shows the 120-bp nucleotide alignment around the der(8) breakpoint. There were no RSS-like sequences on either maternal allele around the breakpoint.

In WILL2, 610 bp of the nucleotide alignment around the der(8) breakpoint (accession no. AB720050) was defined. The 610-bp nucleotides comprised 266 bp of 8q24, 38 bp of N-sequence, and 306 bp of 22q11. The 266 bp of 8q24 perfectly matched the germline sequence. The 306 bp of 22q11 sequence showed thirteen nucleotide substitutions and a 4 bp gap, with a 5.6% difference to the NCBI reference sequence (NG_000002.1). As shown in Fig. 3B, putative RSS was found in both maternal alleles and N-sequence (38 bp) was inserted into the breakpoint. These results suggested that t(8;22)(q24;q11) was a by-product of the *Vλ/Jλ* recombination error.

In KHM10B, 610 bp of nucleotide alignment was determined, encompassing the der(8) breakpoint, consisting of 275 and 335 bp of 8q24 and 22q11, respectively. The 275 bp was fully matched to the germline 8q24 sequence. Putative RSS was found on both maternal 8q24 and 22q11, suggesting that this translocation might result from a *Vλ/Jλ* recombination error (Fig. 3C). There was no N-sequence insertion into the breakpoint. Eight nucleotide mutations were seen in the 335 bp of the 22q11, with 97% match to the *IGλ* germline sequence.

In patient 1, the 391-bp sequence around the der(11) breakpoint (accession no. AB720052) was analyzed. The 153 bp derived from 11q13 contained no nucleotide mutation, whereas the 238 bp derived from 22q11 showed a single-nucleotide mutation and one-nucleotide gap of *Cλ7* with 99% match to the germ line. There was no RSS-like sequence in either maternal chromosome (Fig. 3D).

Molecular cloning of *Vλ/Jλ* rearrangements

LDI-PCR was then performed for *Vλ/Jλ* recombinations. KHM2B, KHM10B, and tumor cells of patient 2 were reported to be positive for surface IGλ, and WILL2 was established from a DLBCL-bearing surface IGλ.